A New, Robust, and Accurate Method to Extract Tide-Coordinated Shorelines from Coastal Elevation Models

Author(s) :Ismael Fernández Luque, Fernando J. Aguilar Torres, Manuel A. Aguilar Torres, José L. Pérez García, and Andrés López Arenas
Source: Journal of Coastal Research, 28(3):683-699. 2012.
Published By: Coastal Education and Research Foundation
DOI: http://dx.doi.org/10.2112/JCOASTRES-D-11-00107.1
URL: http://www.bioone.org/doi/full/10.2112/JCOASTRES-D-11-00107.1

Journal of Coastal Research	28	3	683–699	West Palm Beach, Florida	May 2012

www.cerf-jcr.org

A New, Robust, and Accurate Method to Extract Tide-Coordinated Shorelines from Coastal Elevation Models

Ismael Fernández Luque[†], Fernando J. Aguilar Torres[†], Manuel A. Aguilar Torres[†], José L. Pérez García[‡], and Andrés López Arenas[‡]

[†]Department of Agricultural Engineering
Escuela Superior de Ingeniería
University of Almería
Ctra. Sacramento s/n
041230 Almería, Spain
ismaelf@ual.es
faguilar@ual.es
maguilar@ual.es

[‡]Department of Cartographic Engineering
Geodesy and Photogrammetry
Escuela Politécnica Superior
University of Jaén
Campus de las Lagunillas s/n
23071 Jaén, Spain
jlperez@ujaen.es
alarenas@ujaen.es

www.JCRonline.org

ABSTRACT

FERNÁNDEZ LUQUE, I.; AGUILAR TORRES, F.J.; AGUILAR TORRES, M.A.; PÉREZ GARCÍA, J.L., and LÓPEZ ARENAS, A., 2012. A new, robust, and accurate method to extract tide-coordinated shorelines from coastal elevation models. *Journal of Coastal Research,* 28(3), 683–699. West Palm Beach (Florida), ISSN 0749-0208.

The extraction of highly accurate shoreline data is fundamental to carrying out accurate and reliable studies to enhance our understanding of coastal evolution and coastal vulnerability. In our case, shoreline extraction was needed to develop a method based on an extrapolation process because the most suitable height for datum-coordinated shoreline extraction along Spanish coastal areas turned out to be the orthometric datum origin, *i.e.,* the origin of the vertical reference system in Spain. Because of the microtidal nature of the Mediterranean Sea, using this vertical datum is rather troublesome for remotely extracting ground points to apply to traditional shoreline-extraction methods based on interpolation procedures. Because of these difficulties, a new method for shoreline extraction, based on extrapolation from an iterative digital-elevation model, is presented in this article. The Elevation Gradient Trend Propagation method employs the local elevation gradient to estimate the shoreline position by extrapolating the slope until the zero-elevation contour, representing the modeled intersection of the vertical datum and the beach profile, is reached.

The proposed methodology was tested on a Light Detection and Ranging (LIDAR)–derived digital-elevation model, which comprised a coastal area of Almería (Mediterranean Sea, south Spain). The results obtained from the new approach were compared with those provided by the widely known Cross-Shore Profile (CSP) method.

A validation process was conducted for both methods to highlight their advantages and shortcomings. An alternative contour level of 0.4 m was employed as a ground truth because the zero-elevation contour was not available because LIDAR returns under the water surface were unavailable. The validation process showed that the proposed method was more robust and more suitable than CSP method was for microtidal coasts and for data that need to be extrapolated to reach the desired contour level. In addition, the influence of the starting point in applying the elevation extrapolation process was also proven.

ADDITIONAL INDEX WORDS: *Shoreline change, shoreline detection, shoreline analysis, shoreline definition, coastal erosion–accretion, remote sensing, LIDAR, digital elevation model, extrapolation method, cross-shore profile.*

INTRODUCTION

Mediterranean coastal areas are being progressively degraded mainly because they must withstand high levels of dynamic economic activity from the tourist industry. Moreover, the high profits from these activities are causing new infrastructure (harbors, roads, urbanizations, engineered structures, *etc.*) to emerge, which seriously affects the coastal environment (Suárez and Rodríguez, 2005). Urban development and resource use conflicts in coastal areas can spawn environmental degradation and increase their vulnerability to hazards (Mills *et al.,* 2005). Indeed, coastal areas are some of the richest and changeable, but also most fragile, systems (Woodroffe, 2002). As a result, some specific programs have been developed for the Mediterranean Sea (*e.g.,* United Nations Environment Program/Mediterranean Action Plan) to study the degradation and the conservation processes along Mediterranean coastal areas.

The shoreline, as the reference of land–water interface, is one of the most important features on the Earth's surface, representing a critical indicator of coastal evolution and vulnerability for any Coastal Geographic Information System (Li, Ma, and Di, 2002). Therefore, the development of monitoring techniques to improve the accuracy and efficiency of shoreline mapping is essential to facilitate studies on coastal evolution assessment by estimating the rate of coast erosion or accretion (Aguilar *et al.,* 2010a; Boak and Turner, 2005; Genz *et al.,* 2007).

DOI: 10.2112/JCOASTRES-D-11-00107.1 received 9 June 2011; accepted in revision 23 August 2011.
Published Pre-print online 31 October 2011.

A wide range of geomatic techniques have been employed to extract the shoreline (Boak and Turner, 2005; Gens, 2010). Since the 1920s, aerial photogrammetry has replaced most traditional ground surveys to capture the beach surface by topographic profiling. In recent decades, new technologies have arisen for coast and shoreline mapping, including high-resolution satellite imagery, kinematic Global Positioning System (GPS) vehicles and, above all, airborne LIDAR surveys (Brock and Purkis, 2009). Until recently, the direct digitization of aerial images (orthorectified images are preferred) by identifying a physical shoreline indicator as the high-water line (HWL) has been the most commonly used method (Pajak and Leatherman, 2002). However, because more-accurate spatial data acquisition and analysis techniques have appeared, the set of methods for shoreline definition has increased. Some techniques make it possible to obtain highly accurate, efficient Digital Elevation Models (DEMs), such as Digital Aerial Photogrammetry or airborne LIDAR technology, using datum-coordinated shorelines, based on either tidal or vertical reference datums, as the most suitable shoreline indicator. In fact, a shoreline defined by a stable vertical datum can be treated as a reference shoreline and used to track shoreline changes (Li, Ma and Di, 2002). These types of LIDAR surveys are quite efficient when compared with coastlines extracted by digital orthophotography or photo interpretation because LIDAR-based shorelines are georeferenced to a certain tidal datum, avoiding problems related to biases or horizontal shifts caused by the presence of different tidal levels when the images were taken, the disturbing effects of waves and runup, or even the possible misinterpretations of the wet–dry beach line. Hence, using tidal datum indicators can be deemed a more objective and robust way to identify the shoreline position.

Several methods have been employed in this decade to extract the desired tide-coordinated or datum-coordinated shoreline from LIDAR data. Li, Ma, and Di (2002) described a method of mapping the shoreline by using instantaneous shorelines and other ancillary data; Liu, Sherman, and Gu (2007) devised a method based on morphological operations over segmented LIDAR DEMs; and White (2007) and White *et al.* (2011) proposed a contouring method over LIDAR data by using a datum transformation from geodetic to tidal datums. The latter method is being employed officially by the U.S. National Ocean Service (National Oceanic and Atmospheric Administration, Silver Spring, Maryland). One of the most widespread method for extracting the datum-based shoreline from altimetry data or DEMs is the Cross-Shore Profile (CSP) method (Stockdon *et al.,* 2002), which is based on linear regression over foreshore altimetry profiles. This method has also been used officially by the U.S. Geological Survey (Hapke *et al.,* 2006; Morton and Miller, 2005; Morton, Miller, and Moore, 2004). The adjusted straight line is estimated over a vertical range of heights, and it is intercepted with the desired datum to obtain the shoreline position for each specific profile by using linear interpolation. Tidal datums, such as Mean High Water (MHW) or Mean Lower Low Water (MLLW), are usually employed as the reference for highly accurate, tide-coordinated shoreline extraction (Monmonier, 2008; NRC, 2004) because they correspond to the depth references in nautical charts (MLLW) or include legal boundary considerations (MHW in the United States), and the MHW shoreline provides mariners with a visually recognizable boundary between the land and the sea (Graham, Sault, and Bailey, 2004; Monmonier, 2008). Furthermore, these tidal datums are averaged over a historical record of water-level elevations, embracing a period of not less than 19 years, corresponding to a National Tidal Datum Epoch (NTDE; Ruggiero and List, 2009), so they can be considered robustly computed.

In contrast to the United States, some areas of the Mediterranean coasts (*e.g.,* Spanish coast) lack a large enough network of historical tidal observations to establish an accurate tidal datum. Moreover, the elevation of the MHW tidal datum may experience large variations along the coast as a function of the local tide range and mean tide level. This is the main reason why an open-coast tide station very close to our working coastal area is needed to accurately estimate its MHW, and for the Spanish coast, it is not always available. Therefore, an accurate and easy to define datum should be specified for shoreline extraction along Spanish coast. We strongly recommend the use of the Spanish vertical reference system (orthometric heights). According to Spanish legislation, the vertical reference system in Spain is defined as the mean sea level in the city of Alicante (located on the east side of the Iberian Peninsula, Mediterranean Sea). Actually, this was the first tidal gauge station in Spain, and the mean sea level was recorded from 1870 to 1880. Nowadays, the Spanish vertical reference system is incorporated in the Spanish High-Precision Leveling Network (Red de Nivelación de Alta Precisión [REDNAP]; Instituto Geográfico Nacional, http://www.ign.es). The EGM08 geoid model has recently been adapted to the Spanish Vertical Reference System (REDNAP) with a correction surface adjusted by applying the minimum-curvature algorithm over about 13,700 checkpoints at which both the orthometric and ellipsoid heights were known. Therefore, a reasonably dense geodetic network is currently available in Spain, which allows researchers to locally and accurately establish the EGM08-REDNAP vertical datum throughout the Spanish coast. Furthermore, the observations of the national network of tide gauges are related to this vertical datum (Puertos del Estado, http://www.puertos.es/en), and other geographical features, such as cadastral or administrative information, are also related to this vertical reference level. In fact, the Spanish Oceanography Institute (Instituto Español de Oceanografía [IEO], http://www.ieo.es) defines the 0-m contour level (based on the EGM08-REDNAP orthometric datum) as a required feature for the official geographical database, defining the cartographic element called *shoreline*. That datum-coordinated shoreline can also be applied as a vertical reference for bathymetric works because the *hydrographic zero* (analogous to MLLW datum) is the reference datum for nautical charts in Spain, and many Spanish tidal gauges report a vertical relationship between the EGM08-REDNAP datum and the hydrographic zero (Instituto Hidrográfico de la Marina, http://www.armada.mde.es).

However, choosing the EGM08-REDNAP vertical datum as the most suitable for datum-coordinated shoreline extraction makes it difficult to apply interpolation methods because the instantaneous sea level is, most of the time, located over the corresponding 0-m contour level along the Mediterranean

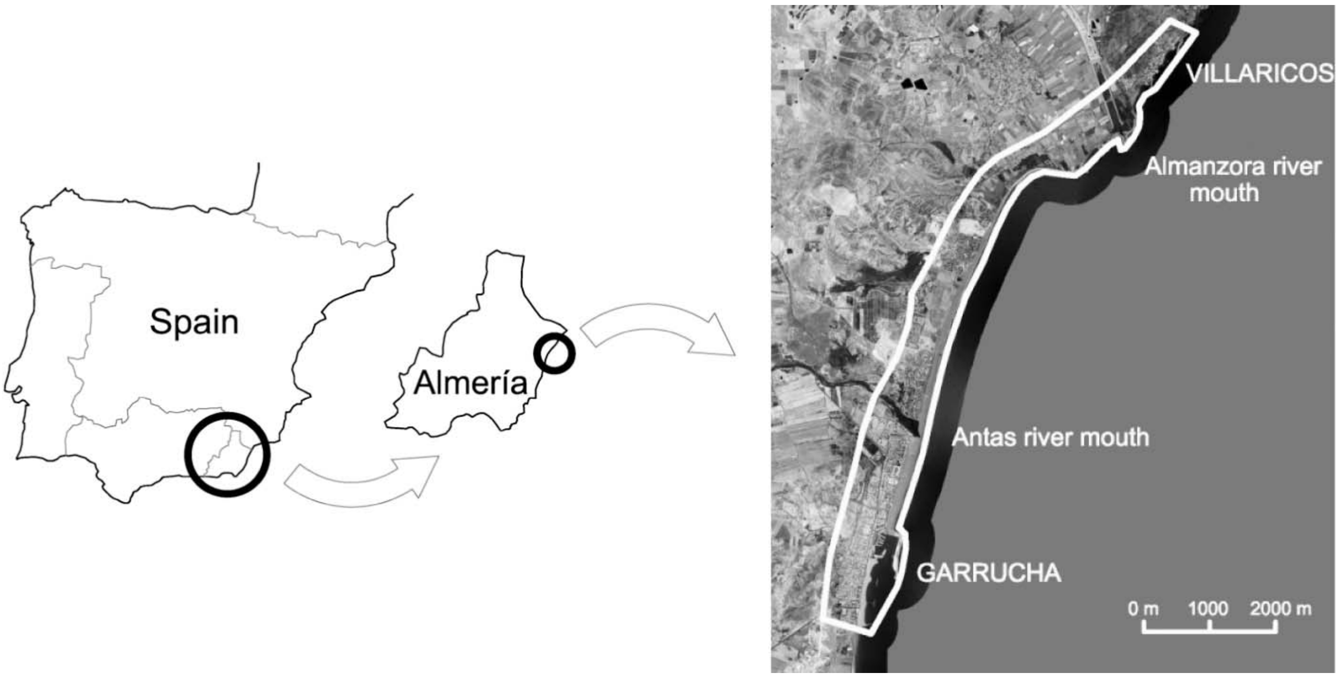

Figure 1. Image of the study site along the Almeria coast (southeast Spain).

Spanish coast. Furthermore, the short tide-level variation and the presence of waves and runup on flat beaches stand in the way of mapping negative elevation data. This makes it very troublesome to count on nearshore bathymetry. Consequently, interpolation methods could be unsuitable for obtaining an accurate zero-elevation shoreline position, and thus, extrapolation methods should be tested.

The main goal of this work was to look for a response to all the aforementioned shortcomings and to outline a new, methodological proposal for high-accuracy shoreline mapping based on DEMs processing and the EGM08-REDNAP orthometric datum as the vertical reference datum. In this way, a new approach for shoreline extraction, the Elevation Gradient Trend Propagation (EGTP), was introduced and tested during this study. This method was based on the iterative extrapolation of the local gradient to obtain the desired zero-elevation contour level (Aguilar *et al.,* 2010a). The new approach was compared with the widespread CSP method because this approach, based on straight-line regression, allows for the application of an extrapolation process. A validation process was conducted on the results from both methods to check which was more suitable for microtidal Mediterranean coastal areas.

DATA SET AND STUDY AREA

The study area was a coastal fringe, 11 km long and 700 m across, on the Mediterranean coast in Almeria province (SE Spain; see Figure 1). From the mid-20th century to the present, this area has undergone heavy coastal erosion. The sedimentary regime of this area is mainly controlled by the Almanzora River, particularly in the study area. The Almanzora River was dammed in 1986, breaking down the sedimentary balance, and accentuating the erosion process. Moreover, this area has undergone increasing anthropic pressure from coastal urbanization and urban sprawl because of the touristic activities. Recently, several seawalls and artificial beach regeneration were created to try to mitigate the beach loss. Therefore, coastal-evolution monitoring and shoreline extraction processes are essential for determining the performance of such as interventions.

The shoreline extraction methods tested within the study area were applied on a 1-m grid spacing, LIDAR-derived DEM taken in August 2009. The flight height aboveground was close to 1000 m, using a Leica Geosystems ALS60 airborne laser scanner with a 35° field of view, 1.61 points/m^2 average point density, and one ground GPS reference station. These data were properly processed to their registration in the ETRS89 geodetic system. The orthometric vertical datum was chosen based on the Spanish vertical reference system (REDNAP, http://www.ign.es/ign/layoutIn/actividadesGeodesiaRedn.do#rednap). The estimated vertical accuracy, computed from 62 Differential Global Positioning System (DGPS), high-accuracy checkpoints distributed throughout the whole study area, took a value of 8.9 cm (measured as standard deviation). All the processes to filter the laser point cloud, adjust the four flight-lines strips, and manage the LIDAR data were conducted with TerraMatch and TerraScan 010 software.

Additionally, TerraScan software allowed the estimation of the instantaneous sea level by plane-to-cloud adjustment at the time LIDAR data were taken because the LIDAR–infrared echo was capable of returns from the water surface on many occasions. In that way, the instantaneous mean sea level was extracted and vertically georeferenced to the Spanish vertical datum, which turned out to be close to an 18-cm average on the open coast, which is almost the locally corrected MHW level estimated from historical data at the tide gauge station located at Almería harbor (non-open coast station), which has a value of about 20 cm. After applying a contouring process to the LIDAR-derived DEM, the 0.4-m contour level was proven to be the most free of noise and outliers from the waves and runup (*i.e.,* it was a continuous contour). As a result, this contour was employed as the reference to filter the LIDAR sea points and to conduct further extrapolation processes (as described further below).

SHORELINE EXTRACTION METHODS

CSP Method

As one of the most extended methods for shoreline extraction based on vertical datum indicators, the CSP method has been implemented as a proper reference for this research (Brock and Purkis, 2009; Hapke *et al.,* 2006; Morton, Miller, and Moore, 2004; Ruggiero and List, 2009; Stockdon *et al.,* 2002). The CSP method, which has been proven suitable for interpolation process (Stockdon et al., 2002), was employed as an extrapolation method throughout this study, which implies that the shoreline position was estimated by supposing that the computed slope from the available data was kept further below the range of the data set

To attain the 0-m datum shoreline with this methodology, the horizontal crossshore profiles were first obtained. The DSAS software (Thieler *et al.,* 2009) was used to achieve an appropriate framework of crossshore profiles or transects (5-m transect spacing) from which the final CSP shoreline was extracted.

By using a 2-m buffer operation on both sides, the corresponding elevation data were included into every cross-profile along the coast. As a result, distances to the profile-origin data (abscise) and the elevation data (ordinate) were recorded for each transect. Then, a regression line was fitted for all profile data with a least-squares method, and the slope and intercept variables were computed. Finally, the intersection between that adjusted line and the chosen water level or reference datum was calculated as shown in Equation (1). Moreover, the covariance matrix resulting from the least-squares adjustment was employed to estimate the uncertainty related to shoreline position for every transect (Wilcox, 2003).

$$x_s = \frac{Z_{datum} - \bar{b}}{\bar{a}} \tag{1}$$

where x_s is the estimated shoreline position with respect to the corresponding profile origin along crossshore axis, Z_{datum} is the datum elevation, $\bar{a}$ is the regression-estimated slope, and $\bar{b}$ is the regression-estimated intercept. Additionally, the linear regression coefficient of determination (R^2) was computed for each profile.

Shoreline Uncertainty Estimation for the CSP Method

Briefly, the relationship between the DEM vertical accuracy of the foreshore slope and the extracted shoreline accuracy (Stockdon *et al.,* 2002) can be explained by

$$\sigma_{XY\ DEM} = \frac{\sigma_Z}{\hat{a}} \tag{2}$$

where $\sigma_{XY\ DEM}$ is the shoreline uncertainty due to vertical uncertainty of the ancillary DEM ($\sigma_z = \pm 0.089$ m in our case). and $\hat{a}$ is the foreshore least-squares estimated slope. However, in addition to the uncertainty proposed by Stockdon *et al.* (2002), the overall uncertainty also depends on the method employed for estimating the shoreline position (Aguilar *et al.,* 2010b), as shown in Equation (3):

$$\sigma_{XY\ TOTAL} = \sqrt{\sigma^2_{XY\ DEM} + \sigma^2_{XY\ regression}} \tag{3}$$

where $\sigma_{XY\ TOTAL}$ corresponds to the total shoreline uncertainty, and $\sigma_{XY\ regression}$ is the uncertainty due to the regression because of the application of the general error propagation law (*e.g.,* Heuvelink, Burrough, and Stein, 1989), yielding Equation (4):

$$\sigma^2_{XY\ regression} = \frac{\sigma^2_a\left(m - \hat{b}\right)^2}{\hat{a}^4} + \frac{\sigma^2_b}{\hat{a}^2} + 2\sigma^2_{ab}\left(\frac{m - \hat{b}}{\hat{a}^3}\right) \tag{4}$$

where σ^2_a and σ^2_b are the variances of computed slope and intercept, respectively, and σ^2_{ab} represents the covariance between both parameters.

Looking for the Best Elevation Range for Applying the CSP Method

An essential parameter for estimating the shoreline position by the CSP method is the proper elevation range. Other authors (*e.g.,* Stockdon *et al.,* 2002) have proposed a general data range of ±0.5 m from the required datum (*i.e.,* the MHW). Because data below the chosen datum in this study were not available, a further study has been carried out to find the most suitable elevation data range from which to start the linear extrapolation process. The 0.2 m and 0.4 m elevations were taken into account as the minimum heights, whereas the tested maximum elevation ranged from 0.8 m to 2.0 m at 0.2-m steps. The potential outliers derived from the CSP shoreline computing process were removed by applying the widely known three-sigma rule (Maune, 2001). The overall results were compared with the decision factor (*DF*) shown in Equation (5). The final chosen range was the range whose results yielded the largest value for the *DF*, which depends on the average of all the computed coefficients of determination $\left(R^2_{average}\right)$, the percentage of data remaining after the outliers are removed ($\%_{remaining\ data}$), and the average estimated uncertainty ($\sigma_{XY\ average}$).

$$DF = \frac{R^2_{average} \times \%_{remaining\ data}}{\sigma_{XY\ average}} \tag{5}$$

In this way, the elevation range from 0.4 m to 0.8 m was found as the best-in-class range for our local conditions. Moreover, the 0.4-m level was proven to be the optimum reference elevation level for applying the extrapolation methods to the DEM data employed in this work because it was perfectly distinguishable against those ranges where the lowest level was 0.2 m (Figure 2). In this last case, waves and runup clearly disturbed the performance of the contouring process by introducing an unacceptable noise.

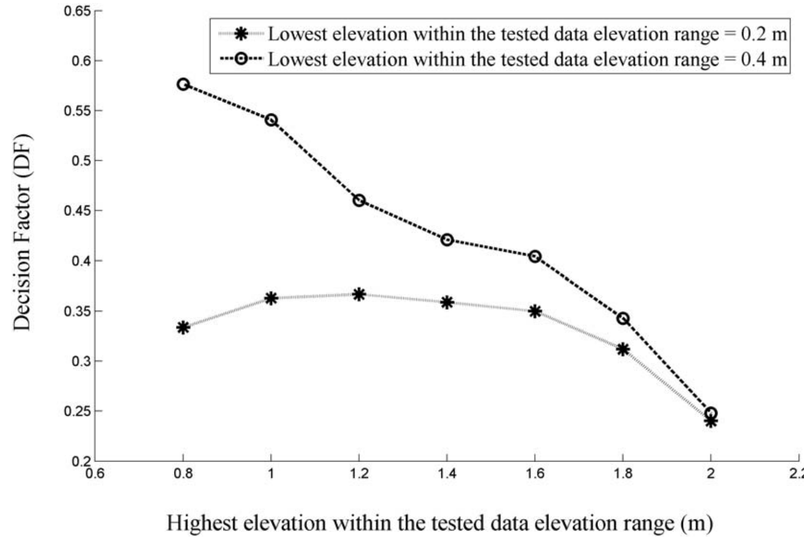

Figure 2. Decision factor (DF) values for each elevation data range tested.

Elevation Gradient Trend Propagation Method

In this study, the EGTP method is proposed as a new approach for shoreline extraction, especially to cope with data and operational conditions where extrapolation is needed. For example, the EGTP method would be useful for those cases where nearshore bathymetry is not available. The EGTP uses an iterative, grid-based data technique that expands the elevation-gradient trend (norm and direction) computed for every grid point toward extrapolated grid points with unknown heights. The process is repeated until the new grid point reaches the level just below the chosen vertical datum. After that, it is easy to join the border that separates the grid points situated above and below the reference height to map the corresponding datum-coordinated shoreline. Obviously, the datum-coordinated shoreline (*e.g.,* EGM08-REDNAP in our case) can be extended to a tidal-coordinated shoreline if a proper tidal datum is available, which should not affect the discussion in the remaining part of the article.

First, elevations below a specific threshold (the reference elevation) are removed. Then, the initial, local gradients and their uncertainty are estimated in an E–W direction (x-axis) and in an N–S direction (y-axis) by means of a Sobel filter (González and Woods, 2008) from the nonremoved elevations as shown in Equation (6):

$$\frac{\partial z}{\partial x} = Gx \cong Z \otimes \begin{bmatrix} -1 & 0 & 1 \\ -2 & 0 & 2 \\ -1 & 0 & 1 \end{bmatrix}; \quad \frac{\partial z}{\partial y} = Gy \cong Z \otimes \begin{bmatrix} -1 & -2 & -1 \\ 0 & 0 & 0 \\ 1 & 2 & 1 \end{bmatrix} \quad (6)$$

where Gx and Gy are the local gradients for the x and y directions, respectively; Z is a 3×3 neighborhood within a grid DEM and $\otimes$ represents the convolution operation. In addition, the estimated, initial gradient uncertainty for both orthogonal directions $\left(\sigma^2_{initial_{Gx}}, \sigma^2_{initial_{Gy}}\right)$ were estimated by applying the general error propagation law (Equation 7):

$$\sigma^2_{initial_{Gx}} = \sigma^2_{initial_{Gy}} = \frac{3}{16r^2}\sigma^2_Z \quad (7)$$

where r is the DEM grid spacing and assuming that it is the same along both the x and y axes.

It is worthwhile to point out that, in every iteration, the elevation gradient for components x and y is only computed for those central grid points that present a complete neighborhood (*i.e.,* all 8 neighbors have a height value). The elevation gradient for each component of those grid points located at the border was interpolated by means of the inverse distance-weighting method, using a local support made up of the gradients actually calculated on the nearest adjacent grid points (Equation 8).

$$Gx_0 = \frac{\sum_{i=1}^{n} Gx_i \times \left(\frac{1}{d_i}\right)}{\sum_{i=1}^{n} \left(\frac{1}{d_i}\right)}; \quad Gy_0 = \frac{\sum_{i=1}^{n} Gy_i \times \left(\frac{1}{d_i}\right)}{\sum_{i=1}^{n} \left(\frac{1}{d_i}\right)} \quad (8)$$

where Gx_0 and Gy_0 are the gradients to be interpolated, i represents each adjacent node where elevation data are known, d_i is the Euclidian distance from each known node to the node to be interpolated, and Gx_i and Gy_i are the gradient values for each adjacent node. Similar to Equation (3), the total gradient uncertainty (given by Equation 10) is estimated by the initial gradient uncertainty (Equation 7) and the uncertainty due to the extrapolation process described in Equation (8). The application of the general error propagation law yields the following expression:

$$\sigma^2_{extr_{Gx}} = \frac{1}{\left[\sum_{i=1}^{n}\left(\frac{1}{d_i}\right)^2\right]}\left[\frac{1}{(d_1)^2}\sigma^2_{initial_{Gx_1}} + \cdots + \frac{1}{(d_n)^2}\sigma^2_{initial_{Gx_n}}\right] \quad (9)$$

$$\sigma^2_{total_{Gx}} = \sigma^2_{initial_{Gx}} + \sigma^2_{extr_{Gx}} \quad (10)$$

where n is the total number of adjacent nodes containing elevation data. Again, the y-axis expression is determined with an analogous method. For the next extrapolation iteration, $\sigma^2_{total_{Gx}}$ would be the initial component, whereas $\sigma^2_{extr_{Gx}}$ would depend on the corresponding variances. In this sense, the actual variance $\sigma^2_{total_{Gx}}$ would increase in each iteration.

An estimation process for extrapolated elevations was carried out once the gradients were computed. The unknown elevations were extrapolated by means of a weighted average onto a 3 × 3 kernel neighborhood. The previously extrapolated gradient results, adjacent node elevations, and relative position regarding the central node are taken into account for the extrapolated elevation estimation (Equation 11).

$$Z_i = \frac{\sum Z + \sum G_x \Delta_i + \sum G_y \Delta_j}{N} \quad (11)$$

In Equation (11), Δ_i and Δ_j are the weighting indexes for the gradients, which make the local gradient additive or subtractive, depending on its relative position with regard to the central node (see Equation 12, where r represents the DEM grid spacing).

$$\Delta_i = \begin{bmatrix} r & r & r \\ 0 & 0 & 0 \\ -r & -r & -r \end{bmatrix}; \quad \Delta_j = \begin{bmatrix} r & 0 & -r \\ r & 0 & -r \\ r & 0 & -r \end{bmatrix} \quad (12)$$

Following the description of the elements of the Equation (11), $\sum z$ is the summation of the adjacent elevations, G_x and G_y are the local gradients corresponding to the 3 × 3 kernel neighborhood, and N is the number of adjacent nodes containing known elevation data. The iterative process is locally stopped when the estimated elevation results are located just below the required vertical datum for shoreline extraction. In our case, the process was stopped when the extrapolated elevations resulted in negative numbers (*i.e.,* below 0 m elevation level). Similar to the gradient process, the elevation uncertainties were also estimated using the following expression:

$$\sigma^2_{total_Z} = \sigma^2_{initial_Z} + \sigma^2_{extr_Z} \quad (13)$$

In this case, $\sigma^2_{initial_Z}$ refers to the initial DEM uncertainty (±0.089 m for the first iteration), and $\sigma^2_{extr_Z}$ indicates the uncertainty caused by the extrapolation process. Again, after applying the general error propagation law through Equation 11, $\sigma^2_{extr_Z}$ could be estimated by means of the next formula:

$$\sigma^2_{extr_Z} = \frac{1}{N^2} \times \sum \left(\sigma^2_{initial_{Z\,ij}} + \sigma^2_{total_{Gx\,ij}} r^2 + \sigma^2_{total_{Gy\,ij}} r^2 \right) \quad (14)$$

where N is the total number of adjacent nodes containing elevation data, $\sigma^2_{total_{Gx\,ij}}$ and $\sigma^2_{total_{Gy\,ij}}$ are the gradient variances at i and j positions (ranging from 1 to 3), and r takes the value of the DEM grid spacing. It is worth noting that grid spacing effectively affects the uncertainty of the extrapolated height, so it is strongly recommended that high-resolution DEMs be used to limit the extrapolation error. Also, notice that the gradient error will be increased after each iteration because of the growing uncertainties in the extrapolated heights.

The last step in the EGTP approach deals with the shoreline contour-level extraction from the final extrapolated DEM. In doing so, the norm and direction of the local elevation gradient are used in the immediately upper elevation of the required datum by means of the horizontal distance from those positions to the required datum. The uncertainty was estimated for both the slope (m) and the horizontal distance (D), as it is shown through the following equations:

$$m = \sqrt{G_x^2 + G_y^2}; \quad \sigma^2_m = \frac{1}{m^2}\left(G_x^2 \sigma^2_{G_x} + G_y^2 \sigma^2_{G_y} \right) \quad (15)$$

$$D = \frac{Z_{ref} - Z_{datum}}{m}; \quad \sigma^2_D = \frac{1}{m^2}\left[\frac{\left(Z_{ref} - Z_{datum}\right)^2}{m^2} \sigma^2_m + \sigma^2_{Z_{ref}} \right] \quad (16)$$

In Equations (15) and (16), G_x and G_y are the gradients in the x and y directions, respectively, and $\sigma^2_{G_x}$ and $\sigma^2_{G_y}$ are their estimated uncertainties along the iterative process. Furthermore, σ^2_m is the slope uncertainty, whereas Z_{ref} and $\sigma^2_{Z_{ref}}$ are the upper elevation for the desired vertical datum elevation and its corresponding uncertainty. Finally, Z_{datum} refers to the shoreline vertical level (0 m, in our case).

The final horizontal coordinates are obtained from the slope direction, the D distance, and the horizontal coordinates of the starting node. Thus, a continuous shoreline can be extracted, usually comprising a large set of shoreline points, one for each pair of contiguous heights vertically located at both sides of the shoreline. Therefore, the denser the original DEM, the more points are available to draw the extracted shoreline.

The shoreline extraction for each CSP transect was conducted to compare the EGTP and CSP methods. In that way, the intersection of each reference transect with the entire shoreline was computed, and, moreover, the average uncertainty between the points A and B was estimated according to the next expression (Li, 1993), where A and B are shoreline points lying on both sides of the resulting intersection point:

$$\sigma^2_{AB} = \frac{1}{3}\sigma^2_A + \frac{1}{3}\sigma^2_B \quad (17)$$

RESULTS AND DISCUSSION

CSP Method Results

As widely proven in other works (Ruggiero and List, 2009; Stockdon *et al.,* 2002), the foreshore slope has a crucial effect on the shoreline accuracy when the CSP method is employed, which can be easily deduced from Equation (2). Furthermore, the data range used to compute the linear regression has been proven very significant. The accuracy is lower and outliers arise when the estimated slope is too small or the elevation data range hardly fits to a straight line, so a further outlier removal process is required. When this sort of errors turns up frequently in a specific area, a dispersion effect appears, and certain coastal areas are clearly ill-defined (*e.g.,* Figure 3). Because a relatively short elevation data range was employed (from 0.4 m to 0.8 m only), the data points used in the fitting procedure

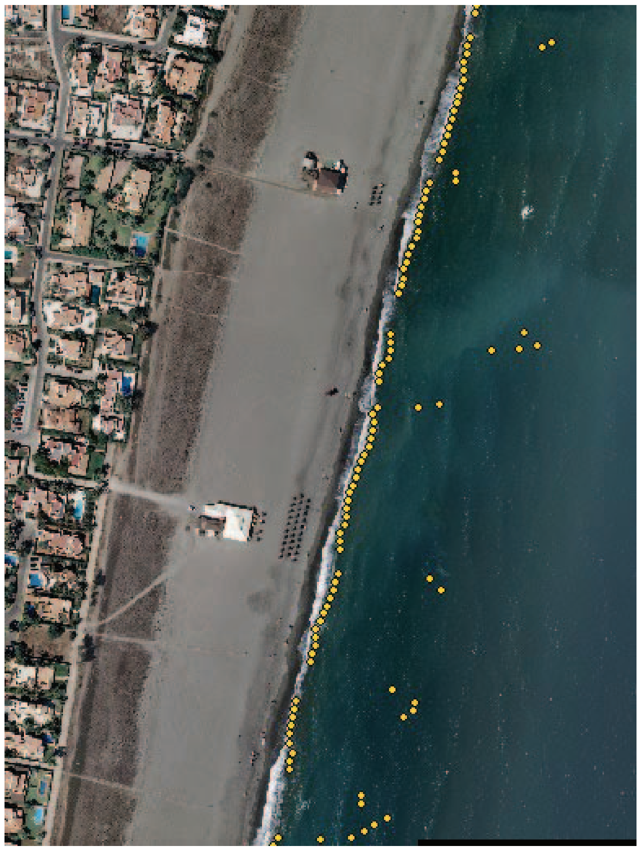

Figure 3. Dispersion effect for the computed shoreline position (yellow points) due to the presence of areas that are too flat (low slope estimation). (Color for this figure is only available in the online version of this paper.)

could be too small and, thus, the relatively high weight applied to any outlier could be worse than the computed least-squares adjustment.

After outlier removal with the three-sigma rule over the entire study area, the maximum uncertainty value was ±10.22 m, the median was ±1.00 m, and the average was ±1.34 m. The number of transects lost was significant, representing the 15% of those initially used. In addition, that the $\sigma^2_{XY\ regression}$, defined in Equation (4), contributed an average of 20% over the $\sigma^2_{XY\ TOTAL}$, depicted in Equation (3). That is, the DEM uncertainty $(\sigma^2_{XY\ DEM})$, was the most influential component of the total uncertainty, although the uncertainty due to the regression term made the model more complete.

The computed theoretical uncertainty for the extracted shoreline seems high (an average of ±1.34 m), although that value should be compared with a proper ground truth because the error from the extrapolation process has to be quantified. For example, the presence of an abrupt change in beach slope and curvature in the immediate vicinity of the datum–shore intersection would produce additional uncertainty not taken into account by the theoretical model.

On the other hand, a clear influence on the final results was attributed to the lack of orthogonality between the shoreline and the transects, which was evaluated with a simple test consisting of checking the effect on shoreline accuracy of different rotations of the transect framework with respect to the shoreline. In fact, the CSP method was applied with a synthetic, required datum of 0.4 m and an elevation data range from 0.6 to 1.0 m in a steady-sloped beach close to 100 m long. The transect system was rotated for the local steepest line from 0° to 75°, at 15° steps. The resulting shoreline for each set of transects was then compared with the ground truth, which was previously extracted as the 0.4 m contour level. The results are depicted in Table 1. As shown, in general, the less the transects and local steepest line are aligned, the greater the extracted shoreline error. Moreover, a systematic bias was found that increased with the increase in the misalignment between the transects and the steepest line.

Table 1. *Residual average and residual standard deviation compared with the ground truth for the different misalignments between transect and steepest line.*

Applied Misalignment (°)	Average Slope	Average R^2	Residual Average (m)	Standard Deviation (m)
0	−0.117	0.981	0.390	±0.287
30	−0.104	0.956	0.337	±0.407
45	−0.05	0.572	−2.506	±1.009
60	−0.05	0.992	1.909	±1.764
75	−0.035	0.523	−4.889	±1.797

EGTP Method Results

The results obtained with the EGTP method have been referenced to the 0.4 m elevation because that has previously been proven to be the most suitable lower contour level. For this iterative approach, the shoreline positions which presented the largest uncertainties did not correspond to any "dispersion effect," but many iterations were needed to achieve the final position. Therefore, no outlier removal process was applied. It is worth noting that a little and limited error appeared as "shoreline gaps," where the local gradient turned out to be positive (*i.e.,* landward) because the extrapolation process was not able to propagate elevations along seaward direction. For the estimated uncertainty, the slope was revealed to be a large influence with the EGTP method as well; generally, the smaller the slope, the larger the number of iterations required and the greater the estimated uncertainties. An average uncertainty of ±2.08 m and a median of ±1.51 m were estimated over the entire study area, which is somewhat larger than that found for the CSP method, but no outliers were removed with the EGTP process.

Qualitative Comparison of CSP *vs.* EGTP

In this study area, the EGTP method was able to represent the shoreline in a more continuous way than was the CSP method. The CSP method was affected by those areas where the elevation data profile was not linear. Moreover, complex and bended coast formations (engineered structures, rocks, little islands, sedimentary shapes, *etc.*) made the CSP method yield irregular results. When the adjusted profiles included outlier data, *i.e.,* wave and runup data, the linear regression

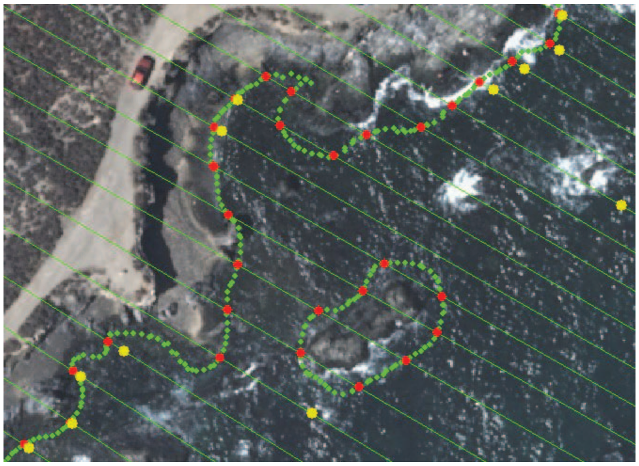

Figure 4. Example of the EGTP method performance for irregular coastal shapes and rocky coastal areas. Green points represent the "continuous" EGTP-derived shoreline, whereas red points depict the EGTP-derived shoreline positions along the transect framework. Yellow points represent CSP-derived shoreline positions. Note that more than one position *per* transect could be captured by the EGTP-derived shoreline. Notice the lack of data and the large errors committed along some transects in the case of the CSP-derived shoreline. (Color for this figure is only available in the online version of this paper.)

was also affected. On the other hand, the EGTP method was more efficient than the CSP method was in representing complex shapes and in drawing the coastal shape properly. In fact, around 14% more transects were available for the EGTP method than were available for the CSP method. Furthermore, the EGTP method was able to identify small islands, yielding more than one position for the same transect, allowing (Figure 4) a more suitable shoreline-evolution analysis over those areas. Additionally, the EGTP method is more automatic and unattended than CSP method because an appropriate elevation data range does not need to be chosen. In fact, the CSP method yielded inappropriate results when small or positive slopes were estimated (Figures 5 and 6), producing an indetermination shoreline along certain coastal areas. Moreover, it was very sensitive to the elevation data range employed, so was most affected in areas of local coast morphology (*e.g.,* berm areas; Figure 7). In such cases, the fit straight line did not correspond to the local, morphological variations. Thus, an important shortcoming of the CSP method is that it requires previous study of the altimetry profiles to find the most suitable elevation data range and to check for fits other than a linear one (Huang, Jackson, and Cooper, 2010). Finally, EGTP method was more independent than was the CSP method regarding the transect framework orientation.

Quantitative Comparison CSP *vs.* EGTP

The high performances of the interpolation processes have been previously proven (Wilcox, 2003). To test the performance of the extrapolation methods applied in this study, a numerical validation process was developed. Because the true 0-m contour level (EGM08-REDNAP required a vertical datum in this study area) was not available because of the absence of a nearshore bathymetry, a synthetic elevation level of 0.4 m was employed as ground truth because it was the first contour level free of unacceptable noise; 14 sample areas were extracted from the DEM, which represented different type of beaches along the study area. In addition, a mixed methodology was proposed to determine the potential negative effect of the transect steepest-line deviation for the CSP method. The mixed method, hereafter called the CSP_EGTP method, was carried out in two steps: (1) an iterative extrapolation of the DEM was applied, similar to that of the EGTP process; and (2) the shoreline was extracted by applying the CSP method over the previously EGTP-extrapolated DEM.

This validation approach was intended to establish the main factors that significantly affect shoreline accuracy. The standard deviation of the differences between the ground truth contour level and the extracted shorelines was employed as an accuracy indicator for each sample area. The tested variables were (1) the method applied (CSP, EGTP, and CSP_EGTP), (2) the reference elevation from which the DEM was extrapolated seaward, and (3) the extrapolated amplitude, *i.e.,* the height difference between the required shoreline extraction level and

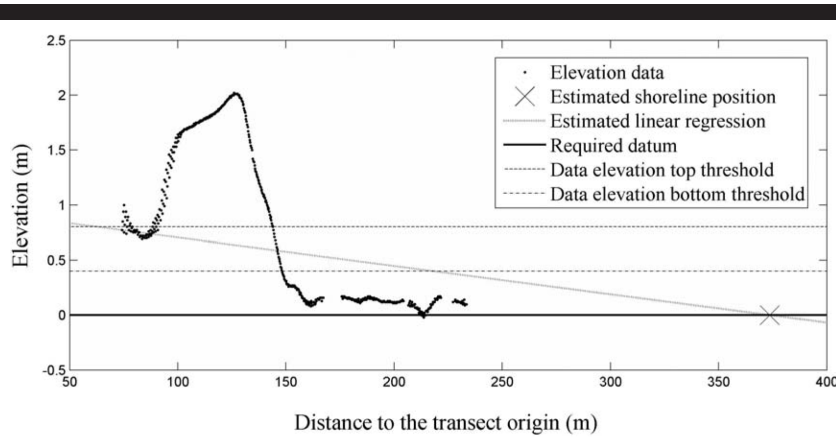

Figure 5. Example of the underestimation of the foreshore slope because of the use of inadequate landward elevation data.

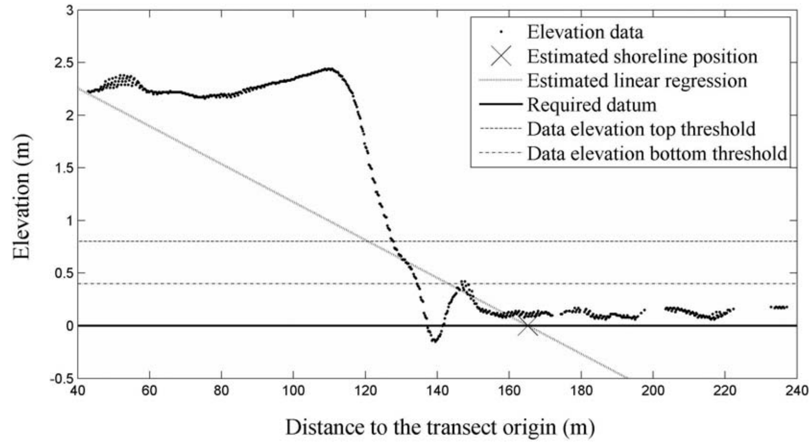

Figure 6. Example of the underestimation of the foreshore slope because of the use of inadequate seaward elevation data.

the reference elevation. Moreover, the extrapolated data range, *i.e.,* the height difference between the minimum and maximum elevation used to compute the regression line in the CSP method, had a value of 0.4 m in every case. The experimental design has been summarized in Table 2.

The results of the standard deviation and the average of the shoreline position differences (random and systematic errors, respectively) for each sample area are shown in Tables 3 and 4. Note that the three-sigma rule for outlier removal was applied to obtain results more suitable for analysis. Certain residual average values could be highly significant, and a systematic error or offset could be likely because of the difference between the extrapolated gradient and the true gradient. This is a bias error inherent to the application of extrapolation approaches, which is usually larger for the CSP method because the EGTP method uses a local gradient that is closer to the true gradient than the one estimated by the CSP method. Tables 3 and 4 show the large variability that exists among the sample sites, which mainly depend on the beach morphology. Significant differences have been found between the EGTP and CSP methods for rocky and highly sloped areas as well as for moderately sloped beaches, where the EGTP method performed better. Furthermore, the transect orientation effect could be tested at some sites. The results from both methods

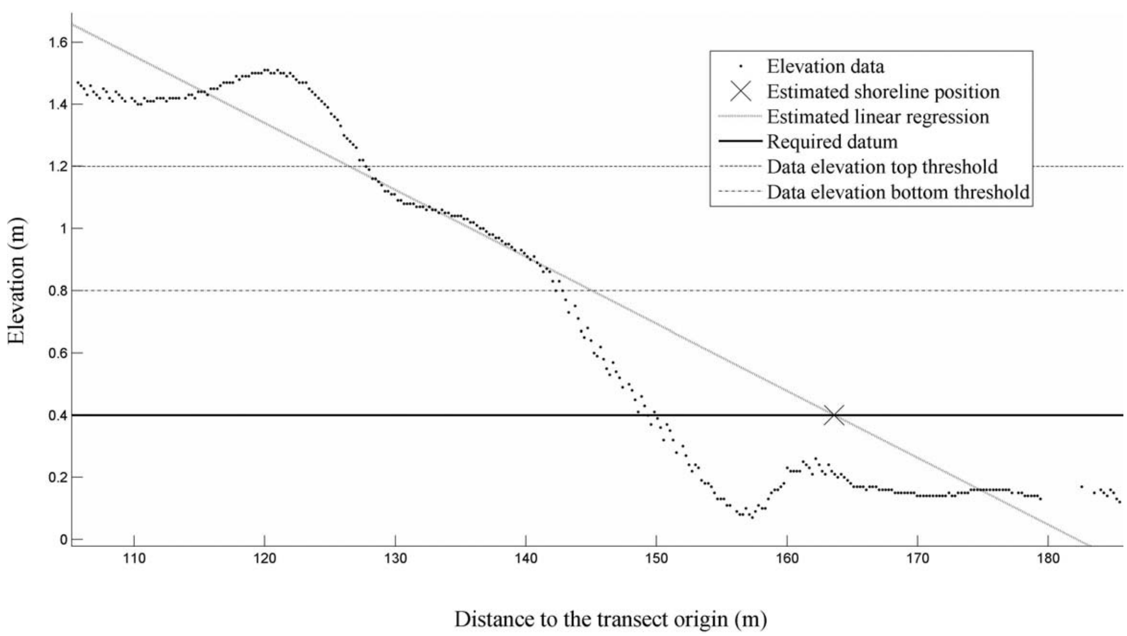

Figure 7. Example of the underestimation of the foreshore slope because of the "berm effect." Note that the required shoreline vertical level is the synthetic 0.4 m one, instead of the 0.0 m level (both referenced to the EGM08-REDNAP vertical datum). The elevation data used in this case ranged from 0.8 m to 1.2 m.

Table 2. *Experimental design for the quantitative analysis conducted to compare the three methods tested.*

Method	Reference Elevation (m)	Extrapolated Amplitude (m)	Elevation Data Range (m)	Alias
EGTP	0.6	0.2	—	EGTP06
EGTP	0.8	0.4	—	EGTP08
EGTP	1.0	0.6	—	EGTP10
CSP	0.6	0.2	1.0–0.6	CSP06
CSP	0.8	0.4	1.2–0.8	CSP08
CSP	1.0	0.6	1.4–1.0	CSP10
CSP-EGTP	0.6	0.2	0.7–0.0	CSP_EGTP06
CSP-EGTP	0.8	0.4	0.9–0.0	CSP_EGTP08
CSP-EGTP	1.0	0.6	1.1–0.0	CSP_EGTP10

were quite similar in beaches with steady slopes (sites 4 and 10). The largest errors were at the so-called nonclassified areas, which corresponded to beach areas where typical berm shapes were present. These bending and irregular shapes negatively affected the results computed with the CSP method when they were embraced by the elevation data range. In this sense, the EGTP method was more robust and less affected by this kind of beach morphology; however, the EGTP method resulted in failures and provided inappropriate results in sample areas where the local gradient was positive or quite low.

Results by Reference Elevation

The influence of the reference elevation can be properly understood if the results for every method tested are separately analyzed. Standard deviation results or extracted shoreline uncertainty highlights the higher accuracy of the EGTP method and how it is affected by the reference elevation (Figure 8). At the reference elevation of 0.6 m (*i.e.,* 0.2 m extrapolated amplitude), the shoreline accuracy is generally under 1 m and rather stable. At 0.8 m, or 0.4 m extrapolated amplitude, the accuracy results were around 1 and 2 m. Note that, for 1.0-m reference level (the highest extrapolated amplitude), the sample sites 8 and 12 have been removed because the extrapolation was erroneous (a positive local gradient). The EGTP values were similar until sample area 5, whereas the results from sample area 6 were usually worse. The offset value clearly grew with the reference elevation. From these results, it can be concluded that the EGTP accuracy clearly depended on the extrapolated amplitude. In fact, the ground truth and the extracted shoreline were quite similar at low amplitudes, whereas the deviations were greater for farther distances, depending on the discrepancy between the modeled foreshore morphology and the true one. Thus, the best reference elevation should be the one as close as possible to the chosen shoreline extraction level to minimize the difference between the true gradient and the extrapolated one.

A better understanding of the performance of each method can be achieved by examining the accuracy results for the reference elevation. The results of the standard deviations for each reference elevation are shown in Figure 9. According to these results, the EGTP method proved more accurate for every reference elevation.

On the other hand, the CSP method seems to be much more dependent on the data range used because the results are usually less accurate than those from the EGTP method. However, the CSP results were appropriate for the 0.6-m reference elevation because they were not affected by the berm effect. In fact, the best accuracy for the CSP method was at the lowest reference elevation (0.6 m), with a general standard deviation close to 2–2.5 m. On the other hand, the results became worse when higher reference levels were used, especially in the berm sites, which can be explained by the foreshore being located within the data range from 0.6 to 1.0 m, whereas most of the berms were at heights greater than 1.0 m. Indeed, that result is proven when compared with other reference elevations, showing that the berm morphology clearly altered the linear foreshore morphology, even more so with the offset results. Therefore, the reference elevation can be highlighted as the main parameter for the CSP method because beach areas have a significant variation in those elevation ranges.

The results for the EGTP and CSP_EGTP methods are quite similar, except for a few sites where the CSP_EGTP was less

Table 3. *Residuals Average results (m) for validating the extrapolated shoreline depending on the observed sample site.*

Sample Site	Group	CSP06	CSP08	CSP10	EGTP06	EGTP08	EGTP10	CSP EGTP06	CSP EGTP08	CSP EGTP10
1	Rocky and highly sloped areas	−1.683	−1.518	−2.316	0.563	0.489	0.557	0.242	−0.246	−0.852
2		−0.713	−1.316	−1.397	0.013	−0.422	−0.488	−0.179	−0.904	−0.888
14		−0.273	−0.074	−0.339	0.125	0.48	0.797	0.04	0.343	0.552
3	Sandy and moderately sloped beach areas	−0.416	−0.766	−1.022	0.414	0.861	1.418	0.315	0.725	1.276
13		−1.643	−5.332	−7.838	−0.271	−1.567	−3.995	−0.358	−1.866	−4.698
4	Sandy and low-sloped beach areas	0.175	−0.991	−0.335	0.418	−0.587	−0.945	0.38	−0.602	−0.142
10		0.782	0.858	0.307	0.643	1.077	0.348	0.609	1.071	0.378
5	Nonclassified areas	−3.499	−2.894	−2.955	−0.645	−2.593*	0.091	−0.659	−2.986*	0.097
6		0.346	−5.07	−6.572	0.432	−0.392	−3.981*	0.407	−0.393	−8.58*
7		0.271	−13.946	−15.805	0.292	−0.812	−6.003*	0.277	−0.809	−5.655*
8		−15.945	−45.159	−13.936	0.436	−1.851	6.35*	0.415	−1.661	28.772*
9		0.563	−2.488	−152.581	0.459	0.905	−1.343	0.429	0.883	−1.591
11		−23.566	−46.553	−128.643	0.17	−0.327	3.079	0.054	−0.892	3.398**
12		−2.44**	−4.785**	−95.73	−1.63	−2.704	4.911*	−1.63	−2.631	−3.826**

*denotes EGTP extrapolation failure due to nonextrapolation of positive gradients; ** denotes results supported by a low number of observations due to the three-sigma outlier analysis.

Table 4. *Standard Deviation results (uncertainty in m) for the extrapolated shoreline validation depending on the observed sample area.*

Sample Site	Group	CSP06	CSP08	CSP10	EGTP06	EGTP08	EGTP10	CSP EGTP06	CSP EGTP08	CSP EGTP10
1	Rocky and highly sloped areas	3.639	3.187	4.159	1.031	1.745	1.718	1.385	2.818	3.562
2		1.168	1.861	2.247	0.587	1.313	1.678	0.792	1.76	1.934
14		1.13	1.807	3.234	0.901	1.444	2.469	0.923	1.41	2.385
3	Sandy and moderately sloped beach areas	0.755	1.447	2.149	0.392	0.705	0.649	0.398	0.635	0.678
13		2.164	3.891	7.12	0.528	1.539	3.869	0.546	1.575	4.113
4	Sandy and low-sloped beach areas	1.193	1.216	1.809	0.857	1.715	1.763	0.84	1.737	1.337
10		0.548	1.223	1.742	0.576	0.959	1.878	0.563	0.948	1.818
5	Nonclassified areas	3.486	2.205	8.638	0.56	1.679*	1.856	0.542	2.034*	2.172
6		0.51	4.584	3.537	0.48	0.92	2.54*	0.466	0.897	7.998*
7		0.468	9.275	5.866	0.382	1.177	2.112*	0.375	1.174	1.893*
8		14.399	38.11	14.695	0.524	1.427	7.852*	0.519	1.434	88.534*
9		0.842	6.72	155.558	0.819	1.202	2.528	0.803	1.198	2.801
11		31.067	59.789	339.387	1.164	3.028	5.78	1.26	4.172	6.592**
12		1.352**	4.467**	101.547	0.805	1.74	16.414*	0.821	2.002	4.123**

* denotes EGTP extrapolation failure due to nonextrapolation of positive gradients; ** denotes results supported by a low number of observations due to the three-sigma outlier analysis.

accurate, which was mainly due to a misalignment between the transect framework and the local steepest line.

Statistical Analysis of the Quantitative Results

To complete the analysis of the aforementioned results, a factorial experimental design was performed. The difference between the estimated shoreline and the ground truth data for each transect was used as the observed or dependent variable. This experimental design allowed us to analyze the influence of different factors and their interactions on the accuracy of the shoreline extraction. The sources of variation studied were sample site, the shoreline extraction method, and the reference elevation, using a factorial univariate analysis of variance (ANOVA) with two dependent-variable grouping levels: (1) individual observations (*i.e.,* each transect as an independent observation), and (2) grouped observations of a given homogeneous sample site. The corresponding uncertainties or standard deviations (as observed variables in the second case) were computed.

ANOVA for the Individual Observations

Table 5 depicts the number of observations for each source of variation: sample site, computation method, and reference elevation. Note that the number of observations for each computation method varied because of the three-sigma outlier analysis, which removed fewer noisy data points observed than did the CSP method, mainly due to its high level of variability when compared with the EGTP and CSP_EGTP methods. In addition, the number of observations was different for each reference elevation because of the larger number of outliers detected and removed in the highest elevation sites.

The final results from the ANOVA study are shown in Table 6. It is worth noting the high significance level for all the factors and their interactions ($p < 0.001$). These results clearly

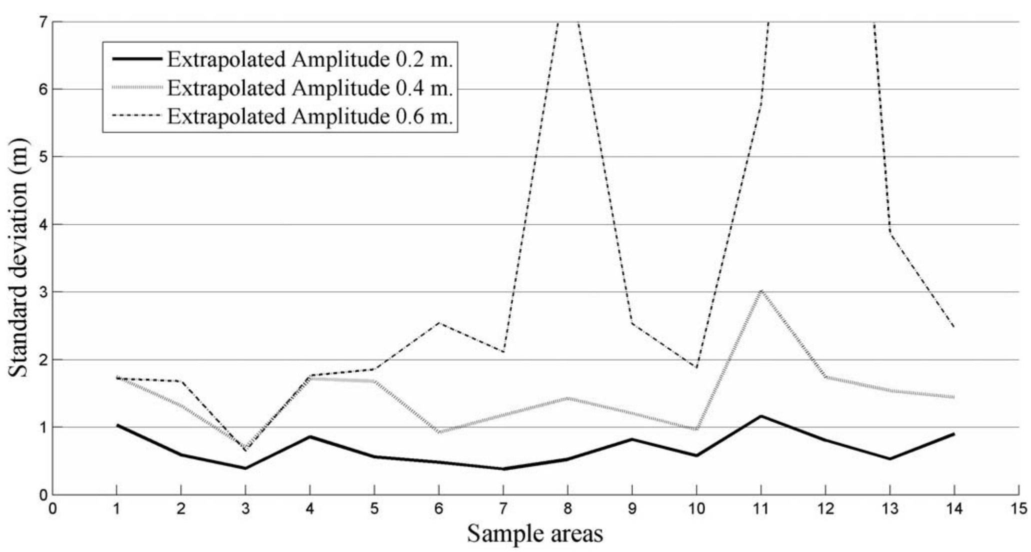

Figure 8. Uncertainty results (standard deviation) for the EGTP method according to the extrapolated amplitude along the different sample sites.

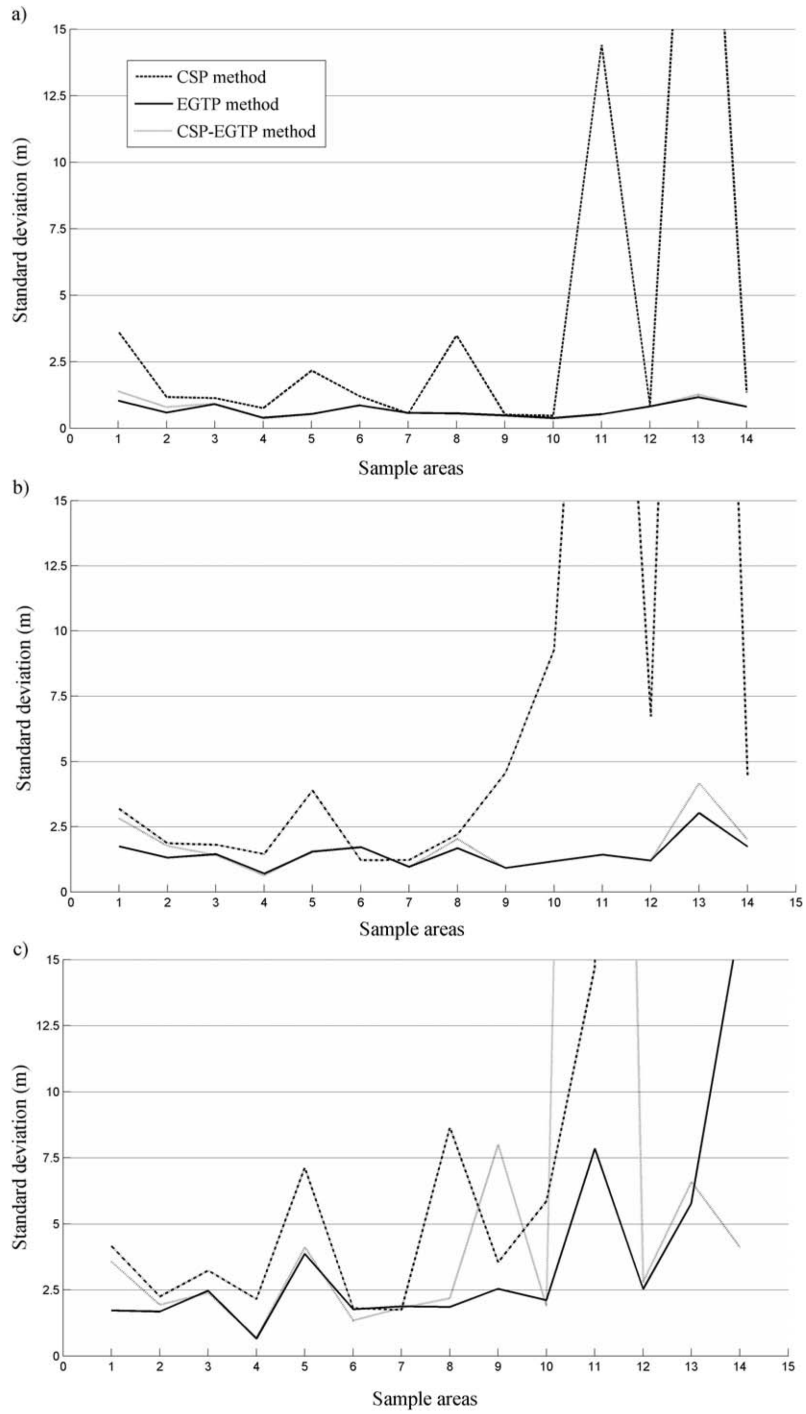

Figure 9. Uncertainty results (standard deviation) for each method tested. (a) Results for the 0.6-m reference elevation or the 0.2-m extrapolated amplitude, (b) results for the 0.8-m reference elevation or the 0.4-m extrapolated amplitude, and (c) results for the 1.0-m reference elevation or the 0.6-m extrapolated amplitude. Note that several results have not been depicted to offer a more understandable representation. These results especially correspond to the CSP method for nonclassified areas (*i.e.,* the sample sites 12–14, in c). See Table 4 for further information.

show that every one of the tested explanatory variables presented a large and statistically significant influence on the final results, as expected. Therefore, the accuracy of the estimated shoreline depends greatly on the extrapolation method applied. In addition, as shown with the qualitative approach, both the sample site and the reference elevation are relevant to shoreline extraction accuracy as well. Meanwhile, the interaction among all the variables was also statistically

Table 5. *Number of observations for each source of variation.*

Factor	Variation	Number of observations
Sample site	1	914
	2	1527
	3	1327
	4	1035
	5	1106
	6	1459
	7	1953
	8	706
	9	1105
	10	2140
	11	826
	12	582
	13	999
	14	972
Computation method	EGTP	5471
	CSP	5741
	CSP_EGTP	5439
Reference elevation	0.6 m	5789
	0.8 m	5600
	1.0 m	5262

significant. For example, each method worked significantly different depending on the sample site to which it was applied, likely because of the presence of different beach morphologies (the interaction of computation method and sample site). The significant interaction of computation method and reference elevation shows that each method yielded different results depending on the reference elevation. Finally, the significant results shown by the interaction of the sample site and reference elevation clearly indicates that every homogeneous area considered, and, therefore, each beach typology, was sensitive to the different reference elevations tested. In this sense, the steadier slopes allowed an increase in the reference elevation and *vice versa*.

Once the results were proven to be statistically significant, a mean separation analysis (MSA) was applied to each factor. In this case, a Tukey's test for treatment differences (John, 1998) was carried out. Tukey's test is a *post hoc* test designed to perform a pairwise means comparison among different levels or treatments corresponding to an analyzed factor, after ANOVA analysis.

The MSA results for the variable sample site are depicted in Table 7. Five clusters were statistically separated; groups 1 and 2 were significantly different, whereas the groups 3–5 are quite underhand. Obviously, the qualitative-based classifications in Tables 3 and 4 do not match the results in Table 7 because these latter results had a *post hoc* analysis applied to differentiate the means in each group, whereas the previous qualitative classification used the standard deviation for each group because that indicated the overall accuracy of the shoreline extraction method applied.

The MSA results for the computation method are depicted in Table 8. This is relevant result because it shows that the EGTP and CSP_EGTP methods were significantly more accurate than the CSP method. In fact, the overall accuracy for the CSP method turned out to be very poor, especially because of the *berm effect* over the profile data adjustment.

The *post hoc* results for reference elevation also turned out to be relevant because they proved that the elevation from which the DEM is extrapolated highly affects the shoreline extraction accuracy. In fact, as it is shown in Table 9, there were three significantly different groups according to the observed variable and the reference elevation, *i.e.,* an increase of only 0.20 m in reference height produced statistically different results in extracted shoreline accuracy, which means the most suitable reference elevation (*i.e.,* as close as possible to the required shoreline extraction level) is needed to start the extrapolation process.

To determine the influence of the CSP method observations on the previous analysis, a further factorial experimental design was conducted with the observed data after removing all the CSP observations. In this case, all factors and interactions were significant ($p < 0.05$), except for the computation method and the interaction of computation method and reference elevation. Therefore, the EGTP and CSP_EGTP methods seemed to achieve quite similar shoreline accuracies. However, a very important finding is shown in Table 10. The *post hoc* results for the reference elevation variable show how the mean value for each level turns out to be much lower than those found in the previous results (Table 9), indicating a polluting effect due to the inclusion of the CSP data. On the other hand, the data was less dependent on the reference elevation because the two highest elevations rendered the same accuracy results.

ANOVA for the Uncertainty (Standard Deviation) Estimated for Each Sample Site

The ANOVA results for individual observations proved that the variables sample site, computation method, and reference

Table 6. *Table of ANOVA results corresponding to the differences between the extracted shoreline and the ground truth along each transect (observed variable).*

Source of Variation	Degrees of Freedom	Sum of Squares	Mean Square	F	Significance($p < 0.05$)
Model	126	6,168,051.49	48,952.79	48.20	**<0.001**
Computation method (A)	2	673,802.05	336,901.02	331.75	**<0.001**
Reference elevation (B)	2	198,285.40	99,142.70	97.62	**<0.001**
Sample site (C)	13	616,843.00	47,449.46	46.72	**<0.001**
A × C	26	1,387,091.31	53,349.66	52.53	**<0.001**
B × C	26	838,015.45	32,231.36	31.73	**<0.001**
A × B	4	468,609.08	117,152.27	115.36	**<0.001**
A × B × C	52	164,7466.52	31,682.04	31.19	**<0.001**
Error	16,525	16,781,593.46	1015.52		
Total	16,651	22,949,644.95			

Bolded values are significant.

Table 7. *Mean separation analysis for the 14 sample sites. Different superscript indices indicate significant differences at* $p < 0.05$.

Sample Site	Homogeneous Groups for Mean Differences (m) for Each Sample Site				
	1	2	3	4	5
11	-23.64^{a}				
9		-18.00^{b}			
12		-15.34^{b}			
8			-6.56^{c}		
7			-4.57^{cd}	-4.57^{cd}	
13			-3.13^{cd}	-3.13^{cd}	-3.14^{cde}
6			-2.49^{cd}	-2.49^{cd}	-2.50^{cde}
5				-1.72^{de}	-1.73^{de}
2				-0.69^{de}	-0.69^{de}
1				-0.49^{de}	-0.49^{de}
4				-0.29^{de}	-0.29^{de}
14					0.29^{e}
3					0.35^{e}
10					0.67^{e}

elevation were statistically significant in explaining the variability in the differences between the estimated shoreline and the ground truth. However, the standard deviation of the aforementioned differences has been established as an adequate accuracy indicator for the extracted shorelines. Therefore, an additional factorial univariate ANOVA was performed over the standard deviation results for each combination of sample site, computation method, and reference elevation. In this case, there were 126 cases or observations (14 sample sites, three computation methods, and three reference elevations).

Table 11 shows the results for the computed standard deviation of the observed differences, where the factors computation method and reference elevation were statistically significant ($p < 0.05$), whereas sample site showed only a slightly significant difference ($p < 0.10$). These results could be anticipated because the number of observations were drastically reduced compared with those used in the first ANOVA to analyze individual observations or transects.

With regard to the *post hoc* analysis for the ANOVA significant factors, a highly relevant finding was obtained from the variables computation method and reference elevation. Two statistically homogeneous groups were separated by Tukey's test for the factor computation method (Table 12). The first group included the CSP method, which was clearly less accurate than the other two methods. There were no significant differences ($p < 0.05$) between the EGTP and CSP_EGTP computation methods for shoreline extraction accuracy.

Regarding the reference elevation variable (Table 13), the *post hoc* analysis highlights two different subsets. The

Table 8. *Mean separation analysis for the three computation methods. Different superscript indices indicate significant differences at* $p < 0.05$.

Computation Method	Mean Values (m) for Each Method	
	1	2
CSP_EGTP		-0.225^{a}
EGTP		-0.174^{a}
CSP	-11.854^{b}	

Table 9. *Mean separation analysis for the three reference elevations. Different superscript indices indicate significant differences at* $p < 0.05$.

Reference Elevation (m)	Mean Values (m) for Each Level		
	1	2	3
0.6			-0.749^{a}
0.8		-2.827^{b}	
1.0	-9.514^{c}		

reference elevations of 1.0 m and 0.6 m were situated within different homogeneous groups, whereas the reference elevation of 0.8 m was not statistically different from the other two elevations. Therefore, the reference elevation to start the extrapolation process significantly affected shoreline extraction accuracy, which was more pronounced when the height difference between the reference elevation and the desired shoreline extraction level was larger.

This quantitative analysis over the transect-by-transect shoreline differences between the extracted shoreline and the ground truth highlights the influence contributed by every variable tested. The extrapolation method was a highly significant factor affecting the variability in shoreline differences, whether by individual observations or by computing their accuracy and standard deviations. The EGTP method was the most suitable method, although there were no significant differences with the CSP_EGTP method. On the other hand, the CSP method was found to be an unsuitable method for extrapolating typical microtidal beach profiles. In addition, reference elevation was established as a decisive parameter because at least two groups could be statistically separated by that parameter, indicating the importance of a proper choice in reference elevation. The nearer the reference elevation is to the shoreline extraction level, the better will be the accuracy of the extracted shoreline. The influence of the data from every sample site can be proven through study of the individual transects, highlighting the existence of a close relationship between the accuracy of the extracted shoreline and the beach morphology.

CONCLUSION

A new methodology based on iterative gradient extrapolation, called the EGTP method, has been presented in this work. It was designed especially for coastal microtidal areas where the required shoreline vertical datum cannot be interpolated because of the absence of data under that level. Moreover, the linear adjustment of altimetry profiles (the CSP methodology) was developed to carry out the extrapolation process, as one of

Table 10. *Mean separation analysis for the two reference elevations after excluding all CSP observations. Different superscript indices indicate significant differences at* $p < 0.05$.

Reference Elevation (m)	Mean Values (m) for Each Level	
	1	2
0.6		0.12^{a}
0.8	-0.37^{b}	
1.0	-0.37^{b}	

Table 11. *Table of ANOVA results corresponding to the standard deviation (dependent variable) computed from individual differences observed for the extracted sample sites.*

Source of Variation	Degrees of Freedom	Sum of Squares	Mean Square	*F*	Significance ($p < 0.05$)
Computation method (A)	2	8549.05	4274.53	4.65	**0.0139**
Reference elevation (B)	2	7931.15	3965.58	4.31	**0.0185**
Sample site (C)	13	21,876.20	1682.79	1.83	0.0628
A × B	4	7395.49	1848.87	2.01	0.1068
A × C	26	39,324.9	1512.50	1.64	0.0636
B × C	26	22,563.6	867.83	0.94	0.5530
Error	52	47,852.00	920.23		
TOTAL	125	155,492.0			

Bolded values are significant.

the most widespread DEM-derived shoreline extraction approaches. The EGTP method usually provided a better drawing of the coastal shapes than did the CSP method, particularly when dealing with bending and complex coastal areas. The influence of transect orientation for an accurate shoreline extraction when using the CSP method has also been proven. Therefore, it is strongly recommended that an automatic profile extraction following the local direction of the steepest line be applied with that method.

In comparison to the CSP algorithm, the EGTP method is presented as a more robust and unattended method, *i.e.,* it is less dependent on onshore data. Furthermore, this new methodology does not need an elevation data range, but only a minimum elevation from which the original DEM is extrapolated. That elevation was 0.40 m in this study, determined after performing a careful DEM contouring inspection, although it could be also be estimated as the maximum wave height or runup (Stockdon *et al.,* 2006) or by removing the LIDAR returns over water (Yates *et al.,* 2008). In addition, this methodology offers a high-resolution shoreline because it is extracted from a method analogous to the contour level, so the EGTP method does not needthe transect framework defined to draw the extracted shoreline, although the transect system is needed to perform a shoreline evolution assessment.

In addition, an exhaustive validation process based on a factorial experimental design was carried out to quantitatively test the performance of the CSP, EGTP, and CSP_EGTP methods. The analysis was carried out using the 0.4-m contour level instead of the required zero-elevation contour (both referenced to the Spanish EGM08-REDNAP vertical datum) because nearshore bathymetric data were not available. In future work, the *in situ* data will be collected (*e.g.,* by DGPS profiles) to carry out a specific validation of the zero-elevation contour corresponding to the Spanish EGM08-REDNAP vertical datum. From this analysis, a systematic error or offset has been detected, which is mainly attributed to the difference between the true gradient and the extrapolated one. Thus, those data that allow interpolation processes to be applied are strongly recommended. The reference elevation was proven to be a statistically significant factor affecting the accuracy of the extracted shoreline, especially with the CSP method. In several areas, the inadequate performance of the CSP method was mostly due to the berm morphology effect, *i.e.,* the captured foreshore profile was not linear. This situation frequently occurred when the elevation data range was highest, so in all likelihood, the berm was relatively high. These results recommend that the ready-to-fit elevation range used should be as close as possible to the required shoreline extraction height. The use of an elevation range below the berm morphology elevation is also recommended.

In summary, satisfactory results were produced with the proposed local gradient extrapolation method for estimating datum-coordinated shorelines where interpolation methods cannot be used. Based on the results of this study, the new grid-based approach can be strongly recommended, both quantitatively and qualitatively, because of its precision, its local slope acquisition, its robustness regarding the presence of noise and outliers, and its capacity to deal with very curved and even closed coastal features.

ACKNOWLEDGMENTS

The authors are very grateful to Andalusia Regional Government (Consejería de Economía, Innovación y Ciencia), Spain, for financing this work through the Excellence Research Project RNM-3575 "Multisource geospatial data integration and mining for the monitoring and modeling of coastal areas evolution and vulnerability: application to a pilot area located at Levante de Almería, Spain." This is a research

Table 12. *Mean separation analysis of the standard deviations for the three computation methods. Different superscript indices indicate significant differences at* $p < 0.05$.

	Homogeneous Groups by Standard Deviation (m)	
Computation Method	1	2
EGTP		1.984^{a}
CSP_EGTP		3.904^{a}
CSP	20.338^{b}	

Table 13. *Mean separation analysis by standard deviation for the three reference elevations. Different superscripted indices indicate significant differences at* $p < 0.05$.

	Homogeneous Groups by Standard Deviation (m)	
Reference Elevation (m)	1	2
0.6		1.966^{a}
0.8	4.385^{ab}	4.385^{ab}
1.0	19.875^{b}	

project cofinanced by the European Union through the European Regional Development Fund (ERDF) Programme.

LITERATURE CITED

Aguilar, F.J.; Fernández, I.; Pérez, J.L.; López, A.; Aguilar, MA.; Mozas, A., and Cardenal, J., 2010a. Preliminary results on high accuracy estimation of shoreline change rate on coastal elevation models. *In: Proceedings of VII Mid-Term International Archives of the Photogrammetry, Remote Sensing and Spatial Information Science Symposium: Networking the World with Remote Sensing* (Kyoto, Japan, ISPRS), pp. 986–991.

Aguilar, F.J.; Mills, J.P.; Delgado, J.; Aguilar, MA.; Negreiros, J.G., and Pérez, J.L., 2010b. Modelling vertical error in LIDAR-derived digital elevation models. *ISPRS Journal of Photogrammetry and Remote Sensing,* 65(1), 103–110.

Boak, E.H. and Turner, I.L., 2005. Shoreline definition and detection: a review. *Journal of Coastal Research,* 21(4), 688–703.

Brock, J.C. and Purkis, S.J., 2009. The emerging role of lidar remote sensing in coastal research and resource management. *In:* Brock, J.C. and Purkis, S.J. (eds.), *Coastal Application of Airborne LIDAR*, Journal of Coastal Research, Special Issue No. 53, pp. 1–5.

Gens, R., 2010. Remote sensing of coastlines: detection, extraction and monitoring. *International Journal of Remote Sensing,* 31(7), 1819–1836.

Genz, A.S.; Fletcher, C.H.; Dunn, R.A.; Frazer, L.N., and Rooney, J.J., 2007. The predictive accuracy of shoreline change rate methods and alongshore beach variation on Maui, Hawaii. *Journal of Coastal Research,* 23(1), 87–105.

González, R.C. and Woods, R.E., 2008. *Digital Image Processing,* 3rd edition. Upper Saddle River, New Jersey: Pearson Prentice Hall, 954p.

Graham, D.; Sault, M., and Bailey, J., 2004. National Ocean Service shoreline: past, present, and future. *In:* Byrnes, M.; Crowell, M., and Fowler, C. (eds.), *Shoreline Mapping and Change Analysis: Technical Considerations and Management Implications,* Journal of Coastal Research, Special Issue No. 38, pp. 14–32.

Hapke, C.J.; Reid, D.; Richmond, B.M.; Ruggiero, P., and List, J., 2006. National assessment of shoreline change, part 3: historical shoreline changes and associated land loss along the sandy shorelines of the California coast. Reston, Virginia: U.S. Geological Survey Open-File Report, 2006-1219, 79p.

Heuvelink, G.B.M.; Burrough, P.A., and Stein, A., 1989. Propagation of errors in spatial modelling with GIS. *International Journal of Geographical Information Systems,* 3(4), 303–322.

Huang, J.D.; Jackson, D.W.T., and Cooper, J.A., 2010. Piecewise polynomial expression of beach profiles. *Journal of Coastal Research,* 26(5), 851–859.

Instituto Español de Oceanografía. IEO Web site. http://www.ieo.es (accessed July 26, 2011).

Instituto Geográfico Nacional. IGN Web site. http://www.ign.es (accessed July 26, 2011).

Instituto Hidográfico de la Marina. Armada Españloa. http://www.armada.mde.es/ArmadaPortal/page/Portal/ArmadaEspannola/ciencia_ihm_1/ (accessed July 26, 2011).

John, P.W.M., 1998. *Statistical Design and Analysis of Experiments*. New York: Society for Industrial and Applied Mathematics, 356p.

Li, R.; Ma, R., and Di, K., 2002. Digital tide-coordinated shorelines, *Journal of Marine Geodesy*, 25(1–2), 27–36.

Li, Z., 1993. Mathematical models of the accuracy of digital terrain model surfaces linearly constructed from square gridded data. *Photogrammetric Record,* 14(82), 661–674.

Liu, H.; Sherman, D., and Gu, S., 2007. Automated extraction of shorelines from airborne light detection and ranging data and accuracy assessment based on Monte Carlo simulation, *Journal of Coastal Research*, 23(6), 1359–1369.

Maune, D.F., 2001. *Digital Elevation Model Technologies and Applications: The DEM Users Manual*. Bethesda, Maryland: American Society for Photogrammetry and Remote Sensing. 539p.

Mills, J.P.; Buckley, S.J.; Mitchell, H.L.; Clarke, P.J., and Edwards, S. J., 2005. A geomatics data integration technique for coastal change monitoring. *Earth Surface Processes and Landforms*, 30, 651–664.

Monmonier, M., 2008. *Coastlines: How Mapmakers Frame the World and Chart Environmental Change*. Chicago: The University of Chicago Press, 228p.

Morton, R.A.; Miller, T.L., and Moore, L.J., 2004. National assessment of shoreline change, part 1: historical shoreline changes and associated coastal land loss along the U.S. Gulf of Mexico. *U.S. Geological Open-File Report* 2004-1043, 45p.

Morton, R.A., and Miller, T.L., 2005. National assessment of shoreline change, part 2: Historical shoreline changes and associated coastal land loss along the U.S. southeast Atlantic Coast. Weston, Virginia: U.S. Geological Survey Open-file Report, 2005-1401. 40p.

NRC (National Research Council), 2004. *A Geospatial Framework for the Coastal Zone: National Needs for Coastal Mapping and Charting*. Washington, DC: National Academy Press, 149p.

Pajak, M.J., and Leatherman, S., 2002. The high water line as shoreline indicator. *Journal of Coastal Research,* 18(2), 329–337.

Puertos del Estado. Puertos del Estado Web site. http://www.puertos.es (accessed May 19, 2011).

REDNAP. Geodesia: La Red Nivelación. http://www.ign.es/ign/layoutIn/actividadesGeodesiaRedn.do (accessed May 19, 2011).

Ruggiero, P. and List, J.H., 2009. Improving accuracy and statistical reliability of shoreline position and change rate estimates. *Journal of Coastal Research,* 25(5), 1069–1081.

Stockdon, H.F.; Holman, R.A.; Howd, P.A., and Sallenger, A.H., Jr., 2006. Empirical parameterization of setup, swash, and runup. *Coastal Engineering,* 53(7), 573–588.

Stockdon, H.F.; Sallenger, A.H., Jr.; List, J.H., and Holman, R.A., 2002. Estimation of shoreline position and change using airborne topographic lidar data. *Journal of Coastal Research,* 18(3), 502–513.

Suárez de Vivero, J.L. and Rodríguez Mateos, J.C., 2005. Coastal crisis: the failure of coastal management in the Spanish Mediterranean region. *Coastal Management,* 33(2), 197–214.

Thieler, E.R.; Himmelstoss, E.A.; Zichichi, J.L., and Ergul, A., 2009. Digital Shoreline Analysis System (DSAS) version 4.0—an ArcGIS extension for calculating shoreline change. Reston, Virginia: U.S. Geological Survey Open-File Report, 2008-1278.

White, S., 2007. Utilization of LIDAR and NOAA's vertical datum transformation tool VDatum) for shoreline delineation. *In: Proceedings of the Marine Technology Society/IEEE OCEANS Conference* (Vancouver, British Columbia, Canada, IEEE), pp. 1–6.

White, S.A.; Parrish, C.E.; Calder, B.R.; Pe'eri, S., and Rzhanov, Y., 2011. Lidar-derived national shoreline: empirical and stochastic uncertainty analyses. *In:* Pe'eri, S. and Long, B. (eds.), *Applied LIDAR Techniques,* Journal of Coastal Research, Special Issue No. 62, pp. 62–74.

Woodroffe, C.D., 2002. *Coasts: Form, Process, and Evolution*. New York: Cambridge University Press, 623p.

Wilcox, R.R., 2003. Least squares regression and Pearson's correlation. *In: Applying Contemporary Statistical Techniques*. San Diego: Academic Press, Elsevier Science, pp. 173–206.

Yates, ML.; Guza, R.T.; Gutierrez, R., and Seymour, R., 2008. A technique for eliminating water returns from LIDAR beach elevation surveys. *Journal of Atmospheric and Oceanic Technology,* 25(9), 1671–1682.

□ RESUMEN □

La extracción de líneas de costa de alta precisión es fundamental para conseguir estudios precisos y fiables dirigidos a entender la evolución costera y su vulnerabilidad. Por ello, existe una necesidad creciente de desarrollar nuevos métodos de extracción de líneas de costa basadas en nivel de mareas donde la línea extraída debe estar georreferenciada a un datum vertical relacionado con un nivel mareal de las aguas. En nuestro caso, fue necesario desarrollar un método basado en procesos de extrapolación ya que el datum más apropiado para la extracción de la línea de costa basada en un nivel de mareas a lo largo de la costa española resultó ser el nivel medio del mar (NMM), es decir, el origen vertical del sistema geodésico español. Debido a la naturaleza micromareal del mar Mediterráneo, este datum vertical está localizado normalmente cercano a pocos centímetros del nivel del mar actual en la costa mediterránea española, lo cual hace que la extracción de puntos del terreno sea problemática bajo este nivel de referencia para aplicar la extracción de líneas de costa basada en procedimientos de interpolación. En este sentido, un método nuevo para la extracción de la línea de costa basado en una extrapolación iterativa del modelo digital de elevaciones se presenta en este trabajo. El método de Propagación de la Tendencia del Gradiente de Elevación (PTGE) emplea la elevación local del gradiente para estimar la posición de la línea de costa extrapolando la pendiente hasta que el datum requerido de elevación es alcanzado.

La metodología propuesta se comprobó en un modelo digital de elevaciones derivado de LIDAR tomado en 2009, el cual se compuso de un área costera de Almería (Mar Mediterráneo, Sur de España) cercano a los 11 km de longitud. Los resultados obtenidos del nuevo método fueron comparados con los proporcionados por el bien extendido método del Cross Shore Profile (CSP).

Se realizó un proceso de validación sobre ambos métodos para averiguar sus ventajas y desventajas. Se empleó para ello un datum alternativo de 0.4 m. como verdad terreno ya que la curva de nivel de 0 m (datum requerido) no se encontraba disponible debido a la falta de retornos LIDAR por debajo de la superficie de las aguas. La validación apuntó que el método propuesto resultó más robusto y apropiado que el método CSP para costas micromareales y cuando existe una necesidad de extrapolación para alcanzar el datum deseado. Además, se comprobó que la altura de partida para aplicar la extrapolación tiene una influencia crucial.